



THE IMPACT OF VEHICLE DENSITY AND DRIVING STYLES ON TRAFFIC FLOW AND CO₂ EMISSIONS

COBISS 1.01

DOI: 10.4312/DZOB1160

Abstract

The purpose of the article is to study the traffic characteristics on a 1500 m long road with one lane and to find out how the flow and carbon dioxide (CO₂) emissions are affected by the density of vehicles, the speed limit, and the way of driving. The research uses a microscopic cellular automaton traffic model (hereafter CA), called the extended LAI model, which contains new functions and is upgraded for the calculation of discharges. Based on the results of traffic simulations, CO₂ emissions per kilometre driven were calculated using the model presented by Panis, Broekx and Liu (2006). The results show that the maximum flow of 2122 vehicles/hour is achieved at a maximum speed of 70 km/h and a density of 0.25 vehicles/cell. Between densities of 0.22 and 0.28 vehicles/cell, the traffic flow is in a synchronized phase, with the average speed dropping due to vehicle interaction. At higher densities, congestion occurs, the average speed continues to fall, and the amount of emissions increases. The top speed only affects CO₂ emissions at lower densities, but at higher densities, they are much more affected by the acceleration rate. We believe that it would be beneficial to reduce traffic density in times of traffic congestion to achieve the most optimal flow and reduce negative impacts on the environment, for example by encouraging occasional work from home, use of public transport, and trips before or after the expected traffic peaks.

Keywords: traffic flow, CO₂ emissions, microscopic traffic flow models, emission models, cellular automata, extended LAI model

*Department of Geography, Faculty of Arts, University of Ljubljana, Aškerčeva cesta 2, SI-1000 Ljubljana, Slovenia (Na jami 16, SI-1000 Ljubljana, Slovenia)

**Chair of Mechanics, Faculty of Civil and Geodetic Engineering, University of Ljubljana, Jamova 508, SI-1000 Ljubljana, Slovenia

e-mail: ar7918@student.uni-lj.si (andrej.rigler1@gmail.com), goran.turk@fgg.uni-lj.si

ORCID: 0000-0002-4596-3594 (G. Turk)

1 INTRODUCTION

Vehicular traffic is a source of different problems, namely, congestions, car accidents, and air pollution. In 2016, the transport sector was responsible for around 25 % of global CO₂ emissions, an increase of 71 % over 1990 levels. Fine particle air pollution can also increase the risk of lung cancer and cardiopulmonary mortality (Escap, 2019; Hoek et al., 2002; Marzoug et al., 2022). The impact of traffic on air pollution is particularly considerable right next to roads. Pollution due to traffic decreases rapidly with distance from roads (Ogrin, 2007; Strle et al., 2020). Location and weather conditions strongly influence the pollution (Glojek et al., 2019). Traffic is also a consumer of space. In cities where noise is also a growing problem, stationary traffic represents a major spatial burden (Ogrin, 2018).

De Vlieger, Keukeleere and Kretzschmar (2000) showed that driving style can reduce traffic emissions and vice versa. Ježek et al. (2015) found that the 25% of diesel-powered passenger vehicles that pollute the environment the most contribute 63 and 47% of black carbon and NO_x emissions, respectively.

For any measures to reduce emissions, it is essential to first assess the emissions. There are two main approaches to emission estimation: macroscopic and microscopic. The former refers to emission estimation at a larger scale, and the latter refers to emissions estimation of each vehicle (Ntziachristos et al., 2009; Panis, Broekx, Liu, 2006; Rakha et al., 2000). Microscopic models calculate emissions from traffic with the help of data on emission factors (EF) of vehicles and their activity. It is a bottom-up approach. There is another way of calculating emissions from traffic, namely “top-down”, where the contributions of sources are determined on the basis of in-situ measurements of the concentrations of various tracers in the ambient air. Ježek (2015) used the tracking method to measure the emission factors of black carbon and NO_x for vehicles of different categories.

While microscopic models are highly accurate, they don't suit large-scale applications. Microscopic models need second-by-second vehicle trajectory data for emission estimation, which requires high computational power. On the other hand, macroscopic models are more computationally efficient for large-scale networks but usually offer lower accuracy, in comparison to microscopic methods. Macroscopic model inputs such as average network speed and density are easy to collect. Loop detectors, already available in many cities and highways, can provide the inputs for macroscopic models (Halakoo, Yang, Abdulsattar, 2023). Microscopic traffic models are necessary to be used in combination with microscopic traffic simulations. They model individual vehicles with realistic traffic flow. Among these, the cellular automata (CA) models are good option to model the traffic flow (Guzman et al., 2018).

The CA models can describe many physical systems and processes. They proved to be useful, not only in traffic flow modeling but also in many different applications, such as the spreading of forest fires, population growth, pedestrian behavior, etc. In

geography, they are used for simulations of land use changes, as they are able to connect the interactions of different factors in space (Pinto, Antunes, Roca, 2021; Xu, Xing Zhu, Liu, 2023). Since CA models calculate the amount of phenomena in space, CA transport models can measure the impact of intersections, road narrowing, speed limits, or other traffic features and factors anywhere in the study area.

A CA model consists of a regular uniform n-dimensional lattice (or array) of cells. Different values of each cell are updated simultaneously at discrete time steps according to the values of its adjacent cells at the preceding time step (Karafyllidis, Thanailakis, 1998; Maerivoet, De Moor, 2005). In the case of the upgraded extended LAI model, the speed, acceleration, and distance traveled of all vehicles are updated simultaneously at each time step.

In the case of traffic CA models, road is discretised into cells of certain size. In single-cell models, each cell is either empty or contains a vehicle. Time is described in discrete time steps, and according to different rules, the states of cells in the system change in time in the sense that it mimics moving vehicles (Maerivoet, De Moor, 2005).

Traffic CA models have become popular in traffic flow modelling due to their efficient and fast performance in computer simulations. Based on a simple set of rules and low computational cost, they can conduct large-scale real simulations. They can also mimic realistic driving behaviour and consider drivers' psychological aspects (Benjamin, Johnson, 1996).

Wolfram's rule 184 is known as the first deterministic traffic flow CA model. It is based on the representation of how a central cell changes in time, depending on two adjacent cells. The physical meaning of the model is that a vehicle moves one step to the right if the space is empty or remains motionless if the space is occupied (Wolfram, 1983).

In 1992, Nagel and Schreckenberg (NaSch) constructed the first stochastic traffic CA model, which includes a stochastic part in one of its rules. With random breaking maneuvers, it can simulate spontaneous traffic jam formation. In the NaSch model, vehicles can speed up only by one level if they have space. The maximum velocity in the NaSch model is 5 (Nagel, Schreckenberg, 1992).

Traffic CA models evolved through time as authors introduced new rules for acceleration, maintaining distance and updating procedure (Barlovic et al., 1998; Benjamin, Johnson, 1996; Knospe et al., 2000; Takayasu, Takayasu, 1993). Kerner, Klenov, and Wolf (2005) made progress by incorporating synchronization distance into their KKW CA model. When a vehicle is within the zone of interaction (i.e., the synchronization distance), it always tries to adjust its speed to the speed of the vehicle in front (Kerner, Klenov, Wolf, 2002).

In 2010, Larraga and Alvarez-Icaza upgraded the CA approach with their LAI model (it is an abbreviation of the authors' names, Larraga and Alvarez-Icaza), which simulates free flow, congested traffic, synchronized flow, and other complex

spatiotemporal patterns. At the same time, the model avoids complex rules, characteristic of models based on the KKW model. In the LAI model, vehicles adjust their speed according to the distance to the vehicle in front of them. Driver's response is based on a safety analysis, which consists of his reaction time, the vehicle's speed, the speed of the vehicle in front, and the gap between them (Larraga, Alvarez-Icaza, 2010). The LAI model was subsequently improved and extended (Guzman et al., 2015; Li et al., 2016).

There are also different microscopic emission models. The model, developed by Panis, Broekx, and Liu in 2018 (PBL model) needs only instant speed and acceleration rate data to calculate PM, VOC, CO₂, and NO_x emissions for urban traffic. The coefficients in the function are obtained from empirical observations. Some models use other data to calculate emissions, such as engine power, road gradient, or vehicle load (Quaassdorff et al., 2022).

Many authors have used a combination of CA models and microscopic emission models. Pan et al. (2018) studied the relationship between traffic flow, fuel rate, dissipation, and particle emissions on a single lane. They used the NaSch CA model for traffic simulations and the PBL model for PM emissions calculation.

Marzoug et al. (2018) studied traffic emissions at signalized intersections. They use the NaSch CA model and a lane-changing model for vehicle movement, traffic light algorithms for signalized intersections, and the PBL model for CO₂, PM, VOC, and NO_x calculation.

Xue et al. (2020) used the KKW three-phase CA model to simulate the traffic flow and study the fuel consumption of vehicles using the method proposed by Treiber, Kesting and Thiemann (2007) on one-way lanes under open boundary conditions. It uses Newton's formula to calculate mechanical power as a function of acceleration and velocity.

The purpose of the article is to study the traffic characteristics on a 1500 m long road with one lane and to find out how the flow and CO₂ emissions are affected by the density of vehicles, the speed limit, and the way of driving. The road is imaginary and does not represent an actual section of the road. By understanding the dynamics of the traffic flow, it is easier to take measures on busy road sections (for example, speed limits, road widening or narrowing, and traffic diversion), which help to reduce the flow and traffic load in the environment. In the Slovenian geographical literature and Slovenian scientific literature in general, we did not find the use of CA models. Although derived from physics, the CA models are also used in geography, especially in the study of land use changes. Also, in the Slovenian literature, we have not seen the invention of a traffic simulator without the use of tools that have already been developed for this purpose. The CA model is suitable for research because it can numerically evaluate a particular phenomenon in time and space. In transport studies, it calculates speeds, accelerations, and locations of vehicles in a unit of time. In combination with the emission model, it is suitable to estimate emissions. At the same time,

it is relatively simple to develop a simulator. The CA model enables performing traffic simulations in relatively large areas. Due to the application of kinematics theory and realistic acceleration and deceleration rates, the extended CA LAI model imitates the actual traffic situation (Guzman et al., 2018).

2 METHODOLOGY

2.1 Traffic component

The model we used in our research is the LAI extended model, which we upgraded to calculate emissions. It originates from the LAI model and its collision avoidance logic that preserves safety. For both models, at each time step, the safe distance of the follower vehicle is calculated according to the speed of the follower vehicle, the speed of the leader vehicle, the emergency braking capability of both vehicles, and the distance between both vehicles. According to the calculated distance, the follower vehicle then decides if it is going to accelerate, keep its velocity, decelerate, or take an emergency braking action.

The authors introduced two novelties in the new version:

1. different limited acceleration and deceleration capabilities for different vehicles,
2. vehicles' acceleration is based on uniform accelerated motion instead of impulsive accelerated motion characteristic for most CA models.

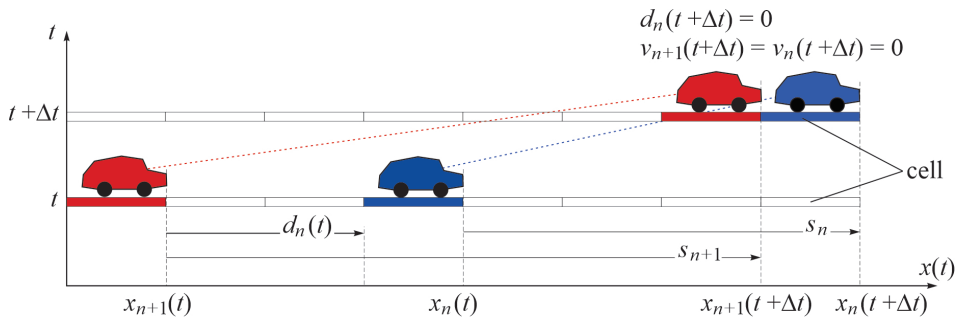
Also, the proposed model calculates three safe distances between vehicles with different driving capabilities. These distances are then used to determine the follower's decision according to the worst-case scenario. However, the improved model is more in line with the realistic traffic than the old one because it uses realistic acceleration/ deceleration rates for the vehicles that approach smoothly to slower or stopped vehicles. Furthermore, it is based on the simple rules of kinematic theory and its parameters according to the neighbors' positions and velocities. The model derives from uniformly accelerated motion, where vehicle state evolution in time is described as follows:

$$x_n(t) = x_{n_0} + v_{n_0}t + \frac{1}{2}a_n t^2 \quad (1)$$

$$v_n(t) = v_{n_0} + a_n t \quad (2)$$

where x_n and v_n denote the position and velocity of the vehicle n , t is time, x_{n_0} and v_{n_0} are the initial position and velocity of the vehicle, respectively, and a_n is the acceleration. Parameter values for accelerations, decelerations and human reaction times derive from real-life observation (Guzman et al., 2018). Therefore, the model overcomes abrupt unrealistic deceleration actions and the complexity of CA models. Simulation results of the LAI extended model show that it can reproduce empirical findings (Guzman et al., 2018).

Figure 1: A schematic diagram for calculating the safe distance.



The LAI extended model is a probabilistic CA model that consists of N vehicles moving in one direction on a one-dimensional lattice of L cells. Each cell is either empty or is occupied by only one vehicle. Their velocities are values that vary from 0 to v_{\max} , which denotes its maximum velocity. Up to this point, there are differences between the LAI extended model and the version used in this research. Namely, in the first model, a vehicle can occupy more than one cell, but in the latter model, it can occupy only one cell. The length of a cell in the later model is 7.5 m, which is the size of a place each car occupies in a complete jam, while the LAI extended model amounts to 1 m (Nagel, Schreckenberg, 1992). Unlike in the LAI extended model, in the new version, the values of velocities are not integer values but real numbers. Regarding the position of a vehicle, two values relate to the vehicle's front bumper. The first value is the exact position of it on the road, and the other is the position that coincides with a sequential number of a cell. The second value is used to calculate emissions. However, except at the beginning, when the vehicle enters the roadway and occupies the entire cell and only one cell, it is later no longer in a single cell. Therefore, the cell value represents the cell that the vehicle entered entirely. The number coincides with a multiplier of the cell size. For example, if the vehicle has the position 7.5 m, it means it has just appeared on the lattice and occupied the first cell. At the position of 14 m, it still occupies the first cell with the remainder of 6.5 m. At position of 15 m, it has just occupied the second cell. There is no possibility that two vehicles would emerge in the same cell because there must be a minimum space gap of a cell size between them. Our upgraded model includes two time variables. The reaction time variable t_r is used to calculate safe distances to determine the new acceleration of a vehicle and is equal to 1 s, which corresponds to human reaction (Guzman et al., 2018).

Based on this acceleration, the other time variable corresponds to the time step Δt used to calculate the updated velocity and the position of a vehicle. Unlike t_r , the variable Δt does not depend on driving styles. This is the second difference with respect to the LAI extended model, which does not include the time variables, because time step and reaction time are always one.

2.2 Updating rules

Step 1:

Safe following distances calculation.

In the first step, the minimum safe following distance for vehicles d_{accn} , d_{keepn} or d_{decn} , is determined, where the variables represent the distances between the leader vehicle n and the follower vehicle $n+1$, if the latter wishes to accelerate, keep its distance, or decelerate, respectively (Guzman et al., 2018).

Step 2:

Slow to acceleration.

According to the vehicle's velocity v_{n+1} , the stochastic noise parameter R_a is determined.

$$R_a = \min \left(R_d, R_0 + v_{n+1} \frac{R_d - R_0}{v_s} \right) \quad (3)$$

where R_a is the stochastic noise parameter, which denotes the probability of accelerating based on the velocity of the vehicle. It is assumed that vehicles whose velocity is smaller than v_s in the previous time step have a lower probability of accelerating than the rest of the moving vehicles $v_{n+1} > v_s$ meaning that slow vehicles must wait longer before they can continue their journey. The stochastic parameter $R_a (< 1)$ linearly interpolates between R_0 and R_d ($R_0 < R_d$) if v_{n+1} is smaller than the velocity v_s , which is in our case 8 m/s (Larraga, Alvarez-Icaza, 2010). All parameter values are defined in the chapter 3.1.

Step 3:

Decision making.

According to the vehicle's space gap $d_n(t)$, compared to previously calculated safety distances in step 1, the follower's acceleration is determined. Acceleration probabilities are also considered (step 2).

Step 3a:

Acceleration.

if $d_{accn} \leq d_n(t)$ then

$$a_{n+1}(t) = \begin{cases} a & \text{if randf() } \leq R_a, \\ 0 & \text{otherwise} \end{cases}$$

where $a_{n+1}(t)$ is the acceleration rate that the follower vehicle will use in the next time step Δt .

Step 3b:

Random slowing down.

if $d_{\text{keep}_n} \leq d_n(t) < d_{\text{acc}_n}$ then

$$a_{n+1}(t) = \begin{cases} -a & \text{if randf() } \leq R_s, \\ 0 & \text{otherwise} \end{cases}$$

where R_s denotes probability of random slowing down despite it has enough space to keep its speed.

Step 3c:

Braking.

if $d_{\text{dec}_n} \leq d_n(t) < d_{\text{keep}_n}$ then

$$a_{n+1}(t) = -a$$

Step 3d:

Emergency braking.

if $d_n(t) < d_{\text{dec}_n}$ then

$$a_{n+1}(t) = -a_{\text{max}}$$

where a_{max} denotes emergency acceleration rate of the follower vehicle.

Step 4:

Action.

$$v_{n+1}(t + \Delta t) = \min(\max(0, v_{n+1}(t) + a_{n+1}(t)\Delta t), v_{\text{max}})$$

where $v_{n+1}(t)$ is the velocity that the follower vehicle uses in the time step t , $v_{n+1}(t+\Delta t)$ is the velocity that the follower vehicle will use in the next time step $t+\Delta t$

Step 5:

Vehicle movement.

if $(a_{n+1}(t) \geq 0)$ then

$$x_{n+1}(t + \Delta t) = x_{n+1}(t) + v_{n+1}(t)\Delta t + \frac{a_{n+1}(t)\Delta t^2}{2}$$

where $x_{n+1}(t+\Delta t)$ is the position of the follower vehicle in the next time step $t+\Delta t$

if ($a_{n+1}(t + \Delta t) < 0$) then

$$x_{n+1}(t + \Delta t) = x_{n+1}(t) + v_{n+1}(t)\Delta t_s + \frac{a_{n+1}(t)\Delta t_s^2}{2}$$

where Δt_s is the time difference between t and the time when the vehicle stops. If this value is less than Δt , Δt_s should be used. The rule is written as follows:

$$\Delta t_s = \min \left(\Delta t, \text{abs} \left(\frac{v_{n+1}(t)}{a_{n+1}(t)} \right) \right)$$

(Guzman et al., 2018).

2.3 CO₂ emission component

In this research, we use the PBL model (Panis, Broekx, Liu, 2006), which allows us to calculate the CO₂ emission of each vehicle at each iteration based on its acceleration (positive or negative) and its instantaneous speed. Panis, Broekx and Liu (2006) showed that this model is appropriate for vehicles' traffic emissions in cities, with a 95 % confidence. Based on empirical measurement and using the multiple non-linear regression technique, they proposed the following general emission function:

$$E_n(t) = \max(E_0, f_1 + f_2v_n(t) + f_3v_n(t)^2 + f_4a_n(t) + f_5a_n(t)^2 + f_6v_n(t)a_n(t)) \quad (4)$$

where $E_n(t)$ is the instantaneous emission (g/s) of vehicle. Variables $v_n(t)$ and $a_n(t)$ are the instantaneous speed and acceleration of the vehicle n at time t . E_0 is a lower limit of emission (g/s) specified for each vehicle and pollutant type, and f_1 to f_6 are emission constants specific for each vehicle and pollutant type. The model can predict CO₂, NO_x, VOC, and PM emissions (Panis, Broekx, Liu, 2006). The PBL model is used in many studies, and it is also the default microscopic emission model in the Aimsun traffic simulator (Halakoo, Yang, Abdulsattar, 2023). The emission constants of the PBL model for CO₂ emissions for petrol and diesel passenger cars are given in Table 1.

Table 1: Parameters for Eq. (4).

Pollutant	Vehicle Type	E_0	f_1	f_2	f_3	f_4	f_5	f_6
CO ₂	Petrol Car	0	$5,53 \cdot 10^{-1}$	$1,61 \cdot 10^{-1}$	$-2,89 \cdot 10^{-3}$	$2,66 \cdot 10^{-1}$	$5,11 \cdot 10^{-1}$	$1,83 \cdot 10^{-1}$
CO ₂	Diesel Car	0	$3,24 \cdot 10^{-1}$	$8,59 \cdot 10^{-1}$	$4,96 \cdot 10^{-3}$	$-5,86 \cdot 10^{-1}$	$4,48 \cdot 10^{-1}$	$2,3 \cdot 10^{-1}$

2.4 The application of CA and PLB methods in geography

The CA transport model method combined with a microscopic emission model, such as the PBL model, is applicable in geographic science primarily because it can measure various phenomena anywhere in the space of study. With the findings, it is then possible to understand traffic phenomena and take measures that would, for example, help reduce its negative environmental impacts. In the case of the research we carried out, the method examines the flow, average speed, and CO₂ emissions on a 1500 m long one-way road depending on various parameters, density, maximum speed limit, and driving aggressiveness. The method also makes it possible to measure other emissions at specific locations, for example, at intersections, traffic lights, pedestrian zones, or larger systems of roads or streets. By determining the flow in different locations, we can also assess other effects of traffic on the environment and make it easier to decide on specific measures helpful for improving the efficiency of traffic.

2.5 Model and parameter settings

The simulation is conducted by Wolfram’s Mathematica software, version 13.2. The model simulates a one-lane circular road with periodic boundary conditions. Each cell represents 7.5 m, and one cell is occupied of a maximum of one car. The determination of the cell size derives from the size of an occupied place by a car in a complete jam (Nagel, Schreckenberg, 1992).

Each time step is $\Delta t = 1$ s. The length of the road $L = 200$ corresponds to the actual road length of 1500 m. In the initial state, the model randomly distributes the vehicles on the road with an initial speed, which is also RANDOMLY selected between 0 and the highest possible speed in relation to the space the vehicle has in front of it. For calculation of the CO₂ emissions, different values for v_{\max} were defined. Eventually, the safety distance estimation, depending on neighboring vehicles, adjusts the maximum velocity by using a quadratic equation, which determines the highest possible speed according to the prerequisite that they are not accelerating at the initial state. In this way, the model is safe and accident-free at the beginning. The density of vehicles on the road amounts to $\rho = \text{vehicle/cell}$. Their velocities and positions are updated according to the rules, described in the methodology chapter. The parameters of the model for the stochastic part are set to the same values as in the LAI extended model $R_d = 1$, $R_0 = 1$, $v_s = 8$ m/s

and $R_s=0.01$. The parameter v_s means that only vehicles with smaller velocity than 8 m/s can accelerate with delay (Guzman et al., 2018).

Defining acceleration and deceleration rates was a more complex task. Based on empirical observations, Guzman et al. (2018) used the value 8 m/s² for the maximum deceleration rate and 4 m/s² for the acceleration rate. In the second part of the study, in which they simulated heterogeneous flow, they used the last values for ordinary vehicles but different values for trucks. Their maximum deceleration rate is (4 m/s²), while their acceleration rate was 2 m/s².

Zeng et al. (2023) used the value 3 m/s² for the acceleration rate. Feng, Liu and Liang (2023) considered different driving styles in their research. According to the information they collected during time measurement on the road section where the maximum velocity was 73.21 km/h, they concluded that 20 % of drivers are aggressive with acceleration and deceleration rate of 4 m/s², 20 % of drivers are calm with acceleration and deceleration rate of 1 m/s², and 60 % of drivers have moderate driving style with acceleration and deceleration rate of 2 m/s².

Based on the collected data, we determined the rate of acceleration for the drivers. We summarized the findings of Feng, Liu and Liang (2023). They concluded that 20% of drivers are aggressive, 60% of drivers are moderate, and 20% of drivers are calm. The aggressive drivers accelerate with an acceleration rate of 4 m/s², calm drivers with 2 m/s², and moderate drivers with 3 m/s². The maximum deceleration rate of aggressive and moderate drivers is 8 m/s², and the one of calm drivers is 4 m/s² (Table 2).

In contrast to Guzman et al. (2018) and Feng, Liu and Liang (2023), the model in this research allows aggressive drivers to accelerate with a lower acceleration rate if they don't have enough space to accelerate with their highest acceleration rate. On the other hand, as in Guzman et al. (2018), they decelerate with only one acceleration rate besides the emergency deceleration rate, which allows aggressive drivers to drive with higher velocity and start decelerating later when they are closer to the vehicle in front. Simulation data for the flow-density, and speed-density diagram, was generated by simulations of 400 seconds. For each density from 0 to 1 10 simulation runs are carried out. The results obtained are then averaged. For the calculation of the CO₂ emissions, different combinations for acceleration and deceleration rates were defined.

Table 2: The parameters of driving styles.

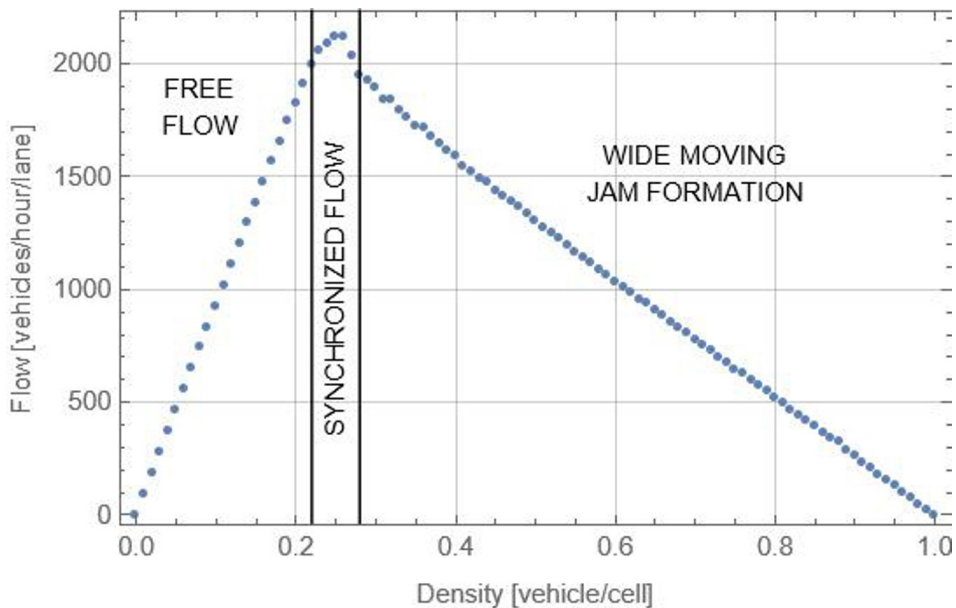
Driving style	Share of Vehicles	Maximum Acceleration	Deceleration	Emergency Deceleration
Aggressive Style	20 %	4 m/s ²	4 m/s ²	8 m/s ²
Moderate Style	60 %	3 m/s ²	3 m/s ²	8 m/s ²
Calm Style	20 %	2 m/s ²	2 m/s ²	4 m/s ²

3 SIMULATION RESULTS AND DISCUSSION

3.1 Fundamental diagram analysis

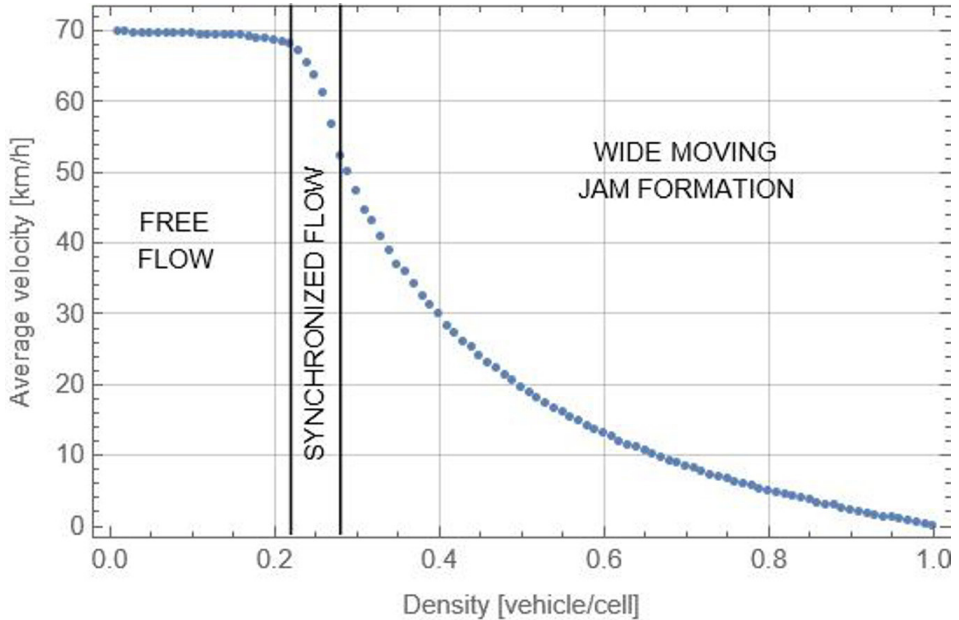
In Figure 2, the flow-density relation of the improved LAI extended model, the so-called fundamental diagram is presented. As seen, the traffic flow reaches its maximum value of 2122 vehicles/hour at the density of 0.25 vehicle/cell, the optimal density above which the traffic flow starts to decrease. Namely, at the density of 0.28, a sudden drop in a traffic flow process occurs and it changes into the congestion phase. The change from the free-flow phase to the synchronized-flow phase occurs at a density of 0.22, when the speed also starts to drop due to more interactions between the vehicles, but no congestion yet occurs. Synchronized flow at the maximum permitted speed of 70 km/h occurs between densities of vehicle/cell.

Figure 2: The flow-density diagram is obtained from the simulations that are carried out in the upgraded LAI extended model for the maximum velocity of 70 km/h.



In Figure 3, the speed-density relation of the improved LAI extended model is presented. It shows that at the synchronized flow region, the average speed drops by 16 km/h from maximum velocity. At the same time, their speed is still stabilized, and vehicles maintain a similar distance between them for the entire road section.

Figure 3: The speed-density diagram is obtained from the simulations that are carried out in the upgraded LAI extended model for the maximum velocity of 70 km/h.



Once the density exceeds 0.27 vehicle/cell, a break-even point is reached with an increase in density of only 0.01. The phase of synchronized flow changes into the phase of congestion (Figure 4c). At a density of 0.28 vehicle/cell, the speed of vehicles is no longer uniform over the entire road section, as congestion starts to appear. Because vehicles maintain a safety distance at a density of 0.28 vehicle/cell, their average speed drops significantly again (Figure 3).

On the other hand, the highest traffic flow in the upgraded LAI extended model at the maximum velocity of 115 km/h is at the density of 0.21 vehicle/cell. The findings are logical because higher speed demands a higher space gap between vehicles. Therefore, at higher speeds, they have enough space at lower densities. The upgraded LAI extended model reaches the highest traffic flow at higher densities than the original LAI extended model of Guzman et al. (2018). We believe it is due to flexible acceleration capabilities that enable vehicles to accelerate at smaller space gaps, although they don't reach the highest acceleration potential.

At different densities, different types of traffic conditions, free flow, synchronized traffic, and wide-moving jams occur as shown in Figure 4. Horizontal rows of dots represent the positions of the vehicles at certain time moving towards the right, while columns of dots represent time instances when the specific cell was occupied by a car. The red and the blue dots represent two specific cars (see also Figure 1).

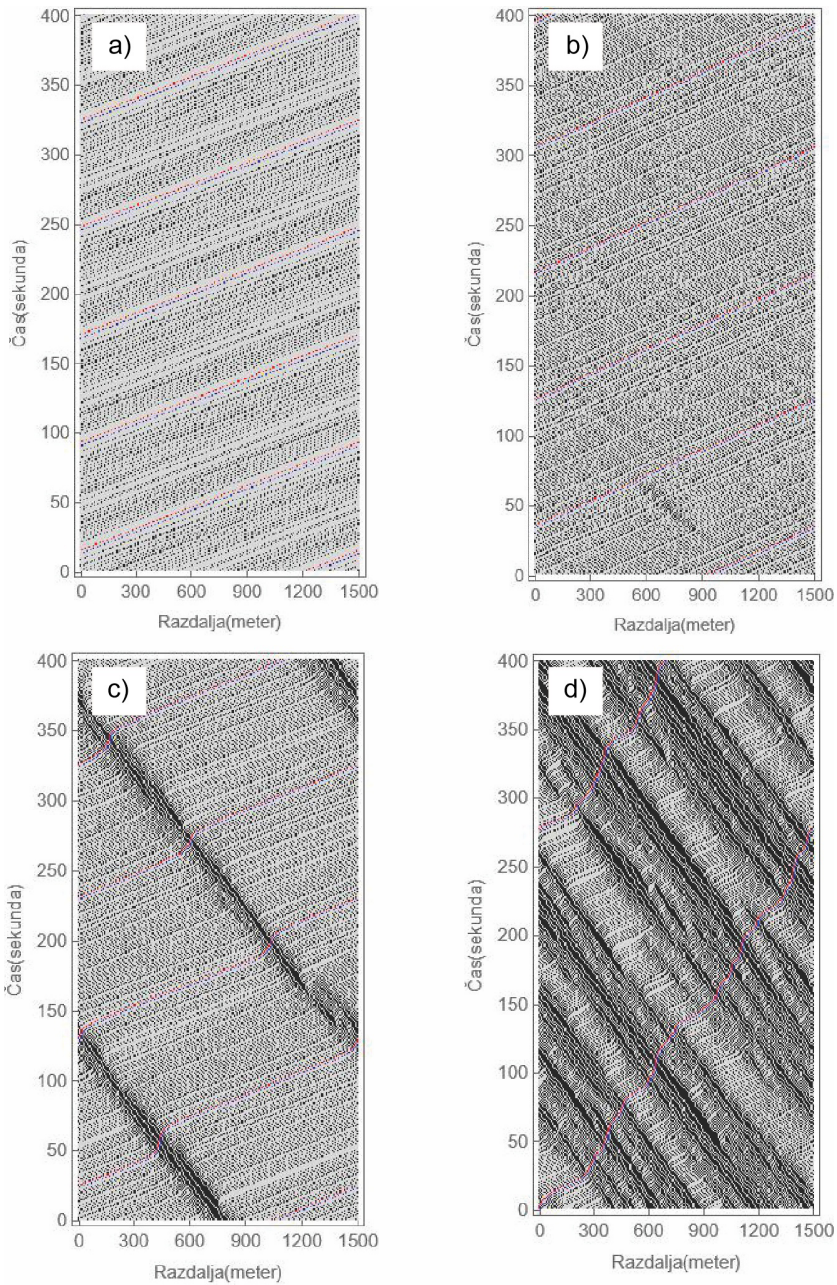


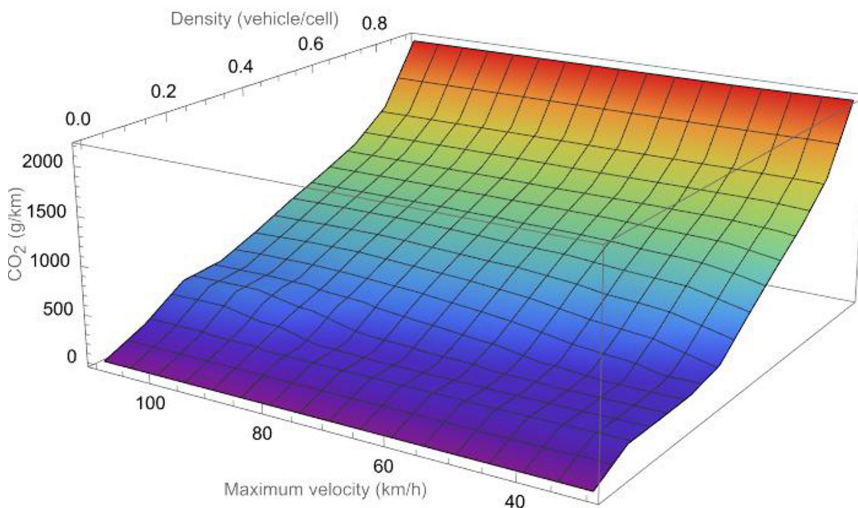
Figure 4: The spatio-temporal diagram of different traffic phases, free (4a), synchronized (4b) and jammed (4c and 4d) for the maximum velocity of 70 km/h.

Vehicles with high speeds when there is no congestion on the road are shown in Figure 4a. Vehicles can take the highest possible speed. When the road is congested, the vehicle's speed drops to zero. Wide-moving jams are shown in the Figure 4c and Figure 4d. The synchronized traffic flow occurs when the speeds drop a little, but the traffic flow is still capable of moving fluidly without jam formation (Figure 4b). Significantly, at the density of 0.27 vehicle/cell, the traffic flow is still in the synchronized phase, but already at 0.28 vehicle/cell, it turns into a jammed phase. Obviously, at the density of 0.27 vehicle/cell, the traffic flow is in the unstable phase because just a slight disorder changes the feature of the flow as is illustrated at the bottom of Figure 4b.

3.2 Impact of the maximum velocity on the CO₂ emissions and traffic flow

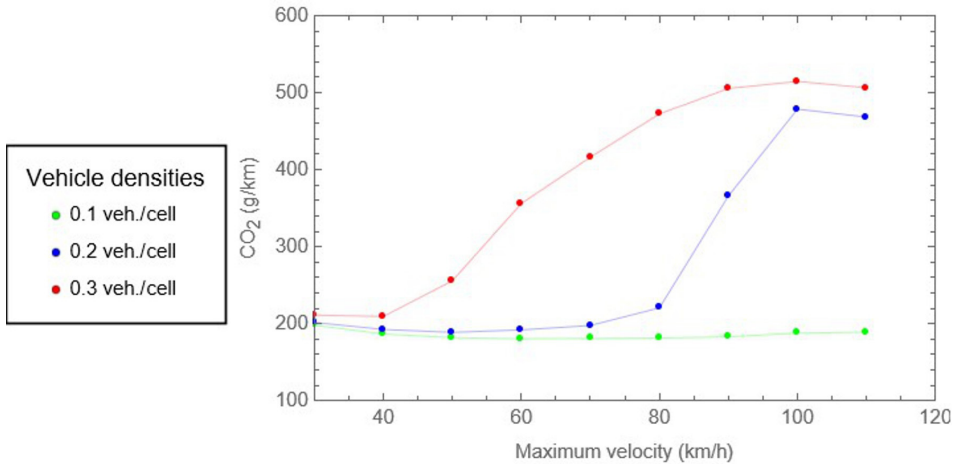
The three-dimensional diagram of CO₂ emissions (in g/km) under different density values (between 0 and 0.9 vehicle/cell) of vehicles and different maximum velocities (between 30 and 110 km/h) is shown in the Figure 5. We calculate the amount of emissions per kilometer driven. Results show that the emission values increase with higher densities. At densities of 0.7 and higher, the emission values are the same for all the maximum velocity values. Namely, the speed does not exceed even the lower maximum velocity threshold (30 km/h). Regardless of the maximum velocity, the velocities remain the same at high densities. At the density values between 0.2 and 0.4, the emission values are more than two times higher for the maximum velocity of 110 km/h than for the maximum velocity of 30 km/h (Figure 6). The reason for this phenomenon is the appearance of congestions, which at these densities occur only at higher speeds.

Figure 5: CO₂ emissions as the function of maximum velocity and density.



The graphs in the Figure 6 show different values of emissions at all studied maximum velocity values at the densities of 0.1, 0.2, and 0.3 vehicle/cell, respectively.

Figure 6: CO₂ emissions as the function of maximum velocity at the densities of 0.1, 0.2 and 0.3 vehicle/cell, respectively.



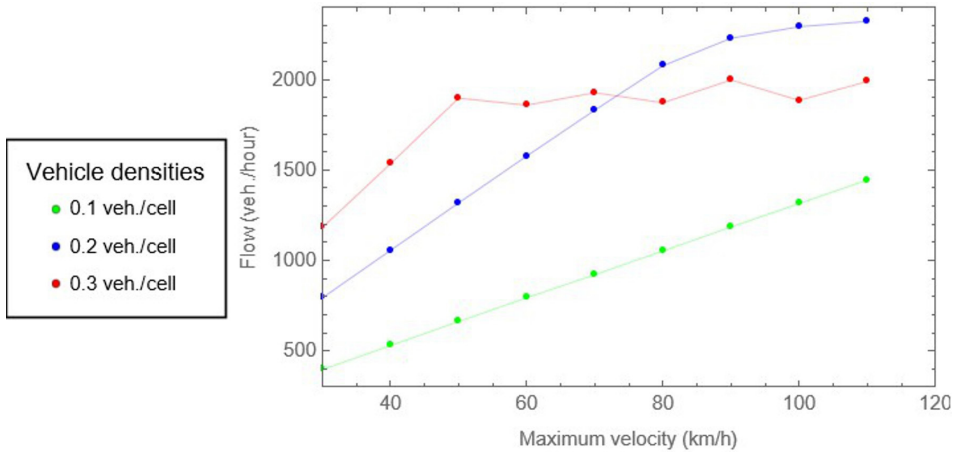
At the density of 0.1, there are no congestions at any maximum velocity value and no influence of congestions. The CO₂ emissions reach the lowest value at the velocity of 60 km/h which corresponds to the lowest emission rate of fuel consumption of some microscale traffic emission models for urban networks (Quaassdorff et al., 2022).

At the density of 0.2 and the maximum velocity of 80 km/h (as evident in the Figure 6), the value of emissions is like the value at the lower maximum velocity values. At the maximum velocity of 90 km/h, the emission value rapidly grows. Therefore, we conclude that at that point, congestions start to occur. At the density of 0.3, the process starts to occur already at lower maximum velocities.

The change of the type of a traffic flow affects the emissions the most, which is seen in the Figure 7. At the density value of 0.2 and maximum velocity values between 80 km/h and 100 km/h, CO₂ emissions more than double, but the traffic flow still grows with the growing maximum velocity at the same parameter values.

At the density value of 0.1, traffic flow grows proportionately with the maximum velocity (Figure 7), but the emissions stay almost constant (Figure 5). It proves that traffic remains at the free flow phase at all studied maximum velocity values. At the density value of 0.3, emissions start to grow rapidly already at the maximum velocity of 50 km/h, and they continue to grow (Figure 6), although traffic flow grows only till the maximum velocity of 50 km/h and then remains similar at higher velocities (Figure 7). It means that at the same density values, more aggressive driving at higher

Figure 7: Traffic flow as the function of maximum velocity at the densities of 0.1, 0.2 and 0.3 vehicle/cell, respectively.



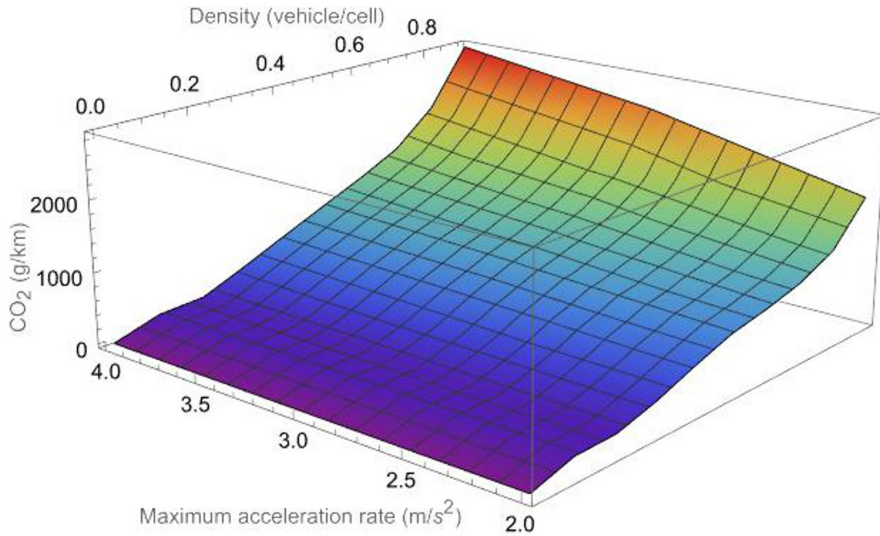
maximum velocity contributes to higher emission values but not higher traffic flow values (also does not contribute to lower traffic flow values). We can conclude that with the change of traffic flow type from free flow to synchronized flow CO₂ emissions start to grow rapidly although the traffic volume stays similar. With the decrease in the traffic flow, CO₂ emissions grow even faster (Figure 5). Namely, more interactions between vehicles contribute to more acceleration and braking and, consequently, higher emissions at similar traffic flow.

3.3 The impact of the maximum acceleration rate on the CO₂ emissions

In the second analysis, we examine the impact of the highest acceleration on the emissions. The three-dimensional diagram of CO₂ emissions (in g/km) under different density values (between 0 and 0.9) of vehicles and different maximum acceleration rates (between 2 and 4 m/s²) is shown in Figure 8. The maximum velocity was constant at 70 km/h. Results show that the higher the density, the larger the difference between the emissions at different maximum acceleration rates.

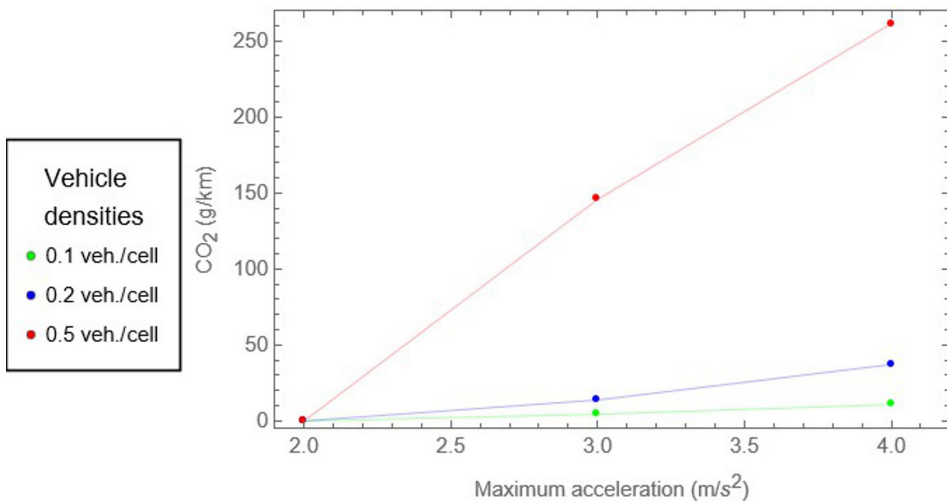
Figure 9 shows different values of emissions at different maximum acceleration rates and densities of 0.1, 0.2, and 0.5, respectively. At the density of 0.1, there are few interactions between vehicles, so they rarely accelerate except when accelerating to the maximum velocity, which they later maintain.

Figure 8: CO₂ emissions as the function of maximum acceleration rate and density.



Aggressive drivers, which tend to accelerate with 4m/s², would contribute to around 6 % more CO₂ emissions than moderate drivers with a maximum acceleration rate of 2 m/s². At the density of 0.2, the percentage grows to 15 %, and at 0.5 to around 33 %. At the density of 0.9, the difference is more than 60 %.

Figure 9: The difference in CO₂ emissions between driving with the highest and the lowest maximum acceleration rate at the densities of 0.1, 0.2 and 0.5 vehicle/cell, respectively.



These differences occur due to a higher frequency of higher acceleration and deceleration rates. It should be noted that aggressive drivers with a higher maximum acceleration rate can accelerate with a lower acceleration rate if they do not have enough space to accelerate with a maximum acceleration rate. On the other hand, they always brake with the same rate of deceleration, which represents the negative value of their maximum rate of acceleration. Both lead to more aggressive driving and consequently large emission values at higher densities when there are more interactions between vehicles.

4 CONCLUSION

As part of the research, simulations of the traffic flow were made to analyze the characteristics of the traffic flow and the influence of different density values on the traffic flow. The influences of the maximum velocity and the maximum acceleration rate by different densities on CO₂ were later discovered. The traffic flow simulations were carried out by the upgraded CA extended LAI model. Traffic CO₂ emissions were later calculated using the PBL microscopic emission model. In the research, we studied the traffic flow with the aim of understanding its characteristics and finding out how to reduce negative environmental impacts on a 1,500 m long single-lane road section, focusing this time on CO₂ emissions. We believe that understanding the internal dynamics of traffic makes it easier and more correct to make decisions about traffic measures.

Fundamental diagrams of traffic flow simulations show that at the maximum velocity of 70 km/h the traffic flow reaches its maximum value of 2122 vehicles/hour at the density of 0.25 vehicles/cell. At 0.28, a sudden drop in the traffic flow process occurs. Before reaching it, the traffic flow starts changing from the free-flow phase to the congestion phase. Up to a density of 0.22, the traffic flow is in the free-flow phase, with the average speed close to the maximum velocity. Between density values of $0.22 < \rho < 0.28$ the traffic flow is in the synchronized phase, when the average speed drops by 16 km/h from maximum velocity. At the same time, their speed stabilizes, and vehicles maintain a similar distance between them for the entire road section. The breaking point occurs when the density > 0.27 with an increase in density of only 0.01. It leads to a change in the traffic flow into a wide-moving jam formation. At that point, the vehicles' speed dropped significantly to maintain safe vehicle distances.

As the traffic density increases from the value of 0.25 vehicle/cell onwards, the traffic flow decreases. Therefore, as the traffic density increases, the traffic flow and speed are further reduced, which increase congestion and CO₂ emissions. It contributes to other negative environmental impacts, such as louder noise, which lasts longer, and higher occupancy of space on roads. It is also worth mentioning the negative economic consequences, as people spend more time in vehicles, causing fatigue and thus making traffic accidents more likely to occur.

Therefore, it would be useful to reduce the traffic density to achieve the most optimal flow or at least prevent further traffic congestion during rush hours. It would increase its efficiency and at the same time reduce negative impacts on the environment. We are aware that transport is a complex system and that significant changes in a short time are difficult to achieve. However, we can already contribute to the prevention of congestion in the short term by possibly avoiding driving during traffic congestion, by occasionally working from home, using public transport, traveling before or after scheduled traffic peaks, and using online applications to choose the most favorable route to avoid traffic jams. Significant changes require long-term planning. More efficient public transport would probably contribute to reducing congestion. Technological solutions are also worth mentioning.

In this research, we determined how CO₂ emissions were affected by the maximum velocity. We concluded that this has the most significant impact between vehicle density values of $0.2 < \rho < 0.4$ when the amount of CO₂ emissions is more than twice as high at the maximum velocity of 110 km/h than at 30 km/h. At the mentioned densities, phase changes in the traffic flow only occur at higher maximum velocity values when the traffic flow changes from free to synchronized. Namely, at a higher maximum velocity, vehicles drive faster when they can, so there are more frequent interactions (acceleration, braking) between vehicles, and the amount of emissions starts to increase rapidly, although the traffic volume remains similar (Figure 6). At the density of 0.1, the traffic is free-flowing at all speeds studied, so there are no significant differences in the amount of emissions. However, at the same density, the flow at the lowest maximum velocity is approximately five times lower than the highest maximum velocity. Therefore, the economic impact of the traffic must also be taken into account. At higher densities, when the traffic flow is in the phase of wide-moving jam formation, simultaneously with the increase in the amount of emissions, the flow decreases at the same time, namely for all speed limits studied. In the long term, the solution would be advanced technology, with the help of which vehicles are connected and tend to drive in platoons. Another measure is again a technological one, namely to change the maximum velocity depending on the traffic density at a specific section.

The influence of emissions due to driving aggressiveness was also discovered namely, at the constant velocity value of 70 km/h and different acceleration. Results show that the higher the density, the larger the difference between the emissions at different maximum acceleration rates. At the density of 0.1, there are few interactions between vehicles, so they rarely accelerate except when accelerating to the maximum velocity. Aggressive drivers, which tend to accelerate with 4m/s^2 , would contribute to around 6 % more CO₂ emissions than calm drivers with a maximum acceleration rate of 2m/s^2 . At the density of 0.2, the difference grows to 15 %, and at 0.5 to around 33 %. At the density of 0.9, the difference is more than 60 %. Therefore, the most environmentally adequate driving is the calm driving with as few impulsive accelerations as possible. So, we suggest encouraging a mild driving style. From the point of view

of the economic impact of traffic, it is not appropriate to drive much slower than the maximum velocity of the particular road section, as this significantly reduces the flow of traffic, especially at lower densities. Transport measures such as the introduction of new bus links, car parks outside city centers, closures of city centers, the introduction of yellow bus lanes, and bicycle rental systems encourage a reduction in the number of vehicles in cities. It contributes to less congestion, increased flow, and lower emissions. Of course, each of these measures would have to be measured to be able to evaluate its effectiveness.

Grant information

Part of the research was financially supported by the Slovenian research Agency (research program P2-0260).

The authors have no relevant financial or non-financial interests to disclose.

References

- Barlovic, R., Santen, L., Schadschneider, A., Schreckenberg, M., 1998. Metastable states in cellular automata for traffic flow, 5, pp. 793–800. DOI: 10.1007/s100510050504.
- Benjamin, S. C., Johnson, N. F., Hui, P. M., 1996. Cellular automata models of traffic flow along a highway containing a junction. Physics Department, Clarendon Laboratory, Oxford University, pp. 1–18. DOI: 10.1088/0305-4470/29/12/018.
- Chowdhury, D., Santen, L., Schadschneider, A., 2000. Statistical physics of vehicular traffic and some related systems. Physics Reports, 329, 4-6, pp. 199–329. DOI: 10.1016/S0370-1573(99)00117-9.
- De Vlieger, I., Keukeleere, D. D., Kretzschmar, G. J., 2000. Environmental effects of driving behaviour and congestion related to passenger cars. Atmospheric Environment, 34, 27, pp. 4649–4655. DOI: 10.1016/S1352-2310(00)00217-X.
- Escap, U., 2019. Using smart transport technologies to mitigate greenhouse gas emissions from the transport sector in Asia. URL: <https://repository.unescap.org/handle/20.500.12870/344> (accessed 08.01.2024).
- Feng, T., Liu, K., Liang, C., 2023. An improved cellular automata traffic flow model considering driving styles. Sustainability, 15, 2, pp. 1–19. DOI: 10.3390/su15020952.
- Glojek, K., Gregorič, A., Ogrin, M., 2019. Black carbon air pollution – case study of Loški Potok. Dela, 50, pp. 25–43. DOI: 10.4312/dela.50.5-43.
- Guzman, H., Larraga, M. E., Alvarez-Icaza, L., 2015. A two lanes cellular automata model for traffic flow considering realistic driving decisions. Journal of Cellular Automata, 10, 1-2, pp. 65–93.
- Guzman, H.A., Larraga, M.E., Alvarez-Icaza, L., Carvajal, J., 2018. A cellular automata model for traffic flow based on kinetics theory, vehicles capabilities and driver reactions. Physica A: Statistical Mechanics and its Applications, 491, pp. 528–548. DOI: 10.1016/j.physa.2017.09.094.

- Halakoo, M., Yang, H., Abdulsattar, H., 2023. Heterogeneity aware emission macroscopic fundamental diagram (e-MFD). *Sustainability*, 15, 2. DOI: 10.3390/su15021653.
- Hoek, G., Brunekreef, B., Goldbohm, S., Fischer, P., van den Brandt, P.A., 2002. Association between mortality and indicators of traffic-related air pollution in the Netherlands: A cohort study. *Lancet*, 360, pp. 1203–1209.
- Ježek, I., 2015. Contribution of traffic and biomass burning to air pollution discriminated with Aethalometer measurements of black carbon. Doctoral thesis. Ljubljana: University of Ljubljana, Faculty of Mathematics and Physics, Department of Physics.
- Ježek, I., Kutrašnik, T., Westerdahl, D., Močnik, G., 2015. Black carbon, particle number concentration and nitrogen oxide emission factors of random in-use vehicles measured with the on-road chasing method. *Atmospheric Chemistry and Physics*, 15, pp. 11011–11026.
- Karafyllidis, I., Thanailakis, A., 1998. A model for predicting forest fire spreading using cellular automata. *Ecological Modelling*, 99, 1. DOI: 10.1016/S0304-3800(96)01942-4.
- Kerner, B. S., Klenov, S. L., Wolf, D. E., 2002. Cellular automata approach to three-phase traffic theory. *Journal of Physics A: Mathematical and General*, 33, pp. 9971–10013. DOI: 10.1088/0305-4470/35/47/303.
- Knospe, W., Santen, L., Schadschneider, A., Schreckenberg, M., 2000. Towards a realistic microscopic description of highway traffic. *Journal of Physics A: Mathematical and General*, 33, pp. 479–485. DOI: 10.1088/0305-4470/33/48/103.
- Larraga, M. E., Alvarez-Icaza, L., 2010. Cellular automaton model for traffic flow based on safe driving policies and human reactions. *Physica A: Statistical Mechanics and its Applications*, 389, 23, pp. 5425–5438. DOI: 10.1016/j.physa.2010.08.020.
- Li, X., Li, X., Xiao, Y., Jia, B., 2016. Modeling mechanical restriction differences between car and heavy truck in two-lane cellular automata traffic flow model. *Physica A: Statistical Mechanics and its Applications*, 451, pp. 49–62. DOI: 10.1016/j.physa.2015.12.157.
- Maerivoet, S., De Moor, B., 2005. Cellular automata models of road traffic. *Physics Reports*, 419, 1, pp. 1–64. DOI: 10.1016/j.physrep.2005.08.005.
- Marzoug, R., Lakouari, N., Perez Cruz, J. R., Vega Gomez, C. J., 2022. Cellular automata model for analysis and optimization of traffic emission at signalized intersection. *Sustainability*, 14, 21. DOI: 10.3390/su142114048.
- Nagel, K., Schreckenberg, M., 1992. A cellular automaton model for freeway traffic. *Journal de Physique I*, 2, 12, pp. 2221–2229. DOI: 10.1051/jp1:1992277.
- Ntziachristos, L., Gkatzoflias, D., Kouridis, C., Samaras, Z., 2009. COPERT: A European road transport emission inventory model. In: Athanasiadis, I. N., Rizzoli, A. E., Mitkas, P. A., Gómez, J. M. (eds.). *Information technologies in environmental engineering*. Springer, pp. 491–504. DOI: 10.1007/978-3-540-88351-7_37.

- Ogrin, M., 2007. Air pollution due to road traffic in Ljubljana. *Dela*, 27, pp. 199–214.
- Ogrin, M., 2018. Prometno obremenjevanje ozračja. V: *Okoljski učinki prometa in turizma v Sloveniji*. Ljubljana: Znanstvena založba Filozofske fakultete, str. 62–72. URL: <https://ebooks.uni-lj.si/ZalozbaUL/catalog/view/60/129/1381> (accessed 08.01.2024).
- Pan, W., Xue, Y., He, H. D., Lu, W. Z., 2018. Impacts of traffic congestion on fuel rate, dissipation and particle emission in a single lane based on NaSch Model. *Physica A: Statistical Mechanics and its Applications*, 503, pp. 154–162. DOI: 10.1088/1748-9326/ac8b21.
- Panis, L. I., Broekx, S., Liu, R., 2006. Modelling instantaneous traffic emission and the influence of traffic speed limits. *Science of The Total Environment*, 371, pp. 270–285. DOI: 10.1016/j.scitotenv.2006.08.017.
- Pinto, N., Antunes, A. P., Roca, J., 2021. A cellular automata model for integrated simulation of land use and transport interactions. *International Journal of Geo-Information*, 10, 3. DOI: <https://doi.org/10.3390/ijgi10030149>.
- Quaassdorff, C., Smit, R., Borge, R., Hausberger, S., 2022. Comparison of microscale traffic emission models for urban networks. *Environmental Research*, 17, pp. 1–15. DOI: 10.1088/1748-9326/ac8b21.
- Rakha, H., Van Aerde, M., Ahn, K., Trani, A., 2000. Requirements for evaluating traffic signal control impacts on energy and emissions based on instantaneous speed and acceleration measurements. *Transportation Research Record*, 1738, pp. 56–67. DOI: 10.3390/ijgi10030149.
- Strle, D., Svetlin, D., Glojek, K., Kobal, M., Pogačnik, K., Ogrin, M., 2020. Meritve koncentracij črnega ogljika in dušikovega dioksida na Lavrici in v Kranju. *Dela*, 54, pp. 5–27. DOI: 10.4312/dela.54.5-52.
- Takayasu, M., Takayasu, H., 1993. $1/f$ noise in a traffic model. *Fractals*, 1, 4, pp. 860–966. DOI: 10.1142/S0218348X93000885.
- Treiber, M., Kesting, A., Thiemann, C., 2008. How much does traffic congestion increase fuel consumption and emissions? applying a fuel consumption model to the NGSIM trajectory data. *TRB 87th Annual Meeting Compendium of Papers*, DVD, pp. 1–17. URL: <https://trid.trb.org/view/848721> (accessed 08.01.2024).
- Wolfram, S., 1983. Statistical mechanics of cellular automata. *Reviews of Modern Physics*, 55, str. 601–644. DOI: 10.1103/RevModPhys.55.601.
- Xu, Q., Xing Zhu, A.X., Liu, J., 2023. Land-use change modeling with cellular automata using land natural evolution unit. *Catena*, 224. DOI: 10.1016/j.catena.2023.106998.
- Xue, Y., Wang, X., Cen, B. L., Zhang, P., He, H. D., 2020. Study on fuel consumption in the Kerner–Klenov–Wolf three-phase cellular automaton traffic flow model. *Non-linear Dynamics*, 102, pp. 393–402. DOI: 10.1007/s11071-020-05947-2.
- Zeng, J., Qian, Y., Li, J., Zhang, Y., Xu, D., 2023. Congestion and energy consumption of heterogeneous traffic flow mixed with intelligent connected vehicles and platoons. *Physica A: Statistical Mechanics and its Applications*, 609, pp. 1–17. DOI: 10.1016/j.physa.2022.128331.